PHYSICAL REVIEW B **66**, 020506(R) (2002)

Mg as a main source for the diverse magnetotransport properties of MgB_2

K. H. Kim, J. B. Betts, M. Jaime, A. H. Lacerda, and G. S. Boebinger
National High Magnetic Field Laboratory, Los Alamos National Laboratory, MS E536, Los Alamos, New Mexico 87545

C. U. Jung, Heon-Jung Kim, Min-Seok Park, and Sung-Ik Lee
National Creative Research Initiative Center for Superconductivity and Department of Physics, Pohang University of Science and Technology, Pohang 790-784, Republic of Korea

(Received 21 November 2001; revised manuscript received 30 April 2002; published 8 July 2002)

Magnetotransport properties of pure Mg metal and MgB_2 samples with varying amounts of unreacted Mg are systematically studied in magnetic fields up to 18 T. With an increasing quantity of Mg, the inhomogeneous MgB_2 samples show a greatly decreased residual resistivity, an enhanced residual resistance ratio (RRR), and enhanced magnetoresistance (MR), gradually approaching the transport behaviors of pure Mg metal. We use the generalized effective medium theory to show that the large RRR and MR of the inhomogeneous MgB_2 samples can be quantitatively explained by a two-phase model in which the two phases are MgB_2 and pure Mg.

DOI: 10.1103/PhysRevB.66.020506 PACS number(s): 74.25.Fy, 74.70.Ad, 74.72.−h, 72.80.Tm

The recent discovery of superconductivity in a binary metallic system MgB_2 with $T_c \approx 39$ K has sparked enormous scientific and technical research efforts.[1] Even though the pairing mechanism was suggested to be of phonon-mediated BCS type,[2] there is no consensus yet even for basic physical properties such as magnetotransport and the magnitude of the superconducting gap.[3] In particular, transport properties of various forms of MgB_2 show very different values of resistivity, residual resistance ratio (RRR), and magnetoresistance (MR).[4–9]

It was generally accepted that a high quality MgB_2 sample should have high RRR (~ 20) and low residual resistivity.[4,5] This is partly related to the so-called Testardi correlation in BCS superconductors,[10] which suggests the highest T_c in the most metallic sample. To explain the diverse transport properties which deviate from low residual resistivity and a high RRR value, various possible origins such as microstrain, insulating impurities, and defect scattering due to off-stoichiometry have been suggested.[7,8] However, three groups recently reported data from single crystals showing the same relatively low value of RRR, ~ 6, in contradiction with the prevailing belief that high quality is linked to high RRR.[11] It is quite important to clarify this issue to understand which are the intrinsic physical properties of MgB_2.

In this communication, we report our magnetotransport study of pure Mg metal as well as a series of MgB_2 samples with varying amounts of Mg. We observed that both pure Mg metal and inhomogeneous MgB_2 samples exhibit large RRR and MR values and small low-temperature (T) resistivity values. Based on the generalized effective-medium theory, we show that the large RRR and MR values can be explained by the magnetotransport properties of Mg.

We use high-pressure synthesis to make high-density-polycrystalline MgB_2 samples with different amounts of unreacted Mg embedded. A Ta capsule containing a stoichiometric mixture of Mg and ^{11}B isotope was heated under 3 GPa in a 12-mm cubic multi-anvil-type press.[7] To control the amount of Mg unreacted inside the MgB_2, the maximum heating T was varied. One batch, A-MgB_2, denotes a sample heated at $\sim 975\,^{\circ}C$ for 2 h. The other two batches, B-MgB_2 and C-MgB_2 were heated at 900 and 850 °C, respectively. The resulting samples were characterized with magnetization, scanning electron microscopy (SEM), and x-ray diffraction (XRD).

According to the XRD data, A-MgB_2 does not have any appreciable impurities. However, unreacted Mg and a small amount of MgO impurity (2–5 %) were identified in the XRD profiles of B-MgB_2 and C-MgB_2, while unreacted B_2 was not observed within the resolution of the XRD data. The SEM study showed that A-MgB_2 has well-connected grains without any clear distinction of grain boundaries. The images of B- and C-MgB_2 indicated that they are inhomogeneous phase mixtures, mainly composed of pure MgB_2 and Mg with grain sizes as large as ~ 100 μm (the inset of Fig. 3), as confirmed by energy dispersive spectra.[12] From the SEM pictures, the area of the Mg grains in B-MgB_2 and C-MgB_2 were estimated to be $16.7 \pm 2\%$ and $29.0 \pm 1\%$ of a total sample area, respectively. Details of the sample growth and characterization were reported elsewhere.[12]

We measured the T- and magnetic-field (H)-dependent resistivity $\rho(T,H)$ of the three MgB_2 samples as well as commercial Mg metal (Alfa Aesar #43355, 99.9%), using the standard four-probe method in a cryostat equipped with an 18-T superconducting magnet. In all the measurements, electrical current was applied perpendicular to the magnetic field. The bar-shaped MgB_2 specimens were typically $0.5 \times 1 \times 4$ mm^3 and the Mg metal was $1.2 \times 1.3 \times 5$ mm^3. The errors of resistivity, ρ, due to geometry are estimated to be less than 10%.

Figure 1 displays $\rho(T,H)$ of A-, B-, and C-MgB_2, and Mg at 0, 5, 10, 12, 15, and 18 T in a T range between 3 and 300 K. The A-MgB_2 sample shows the highest $T_c = 38.8$ K (midpoint) and the smallest transition width $\Delta T_c \approx 0.3$ K, based on a 10–90 % criterion of ρ value. The $\rho(T,H=0)$ of this sample at 40 and 300 K were 5.14 and 30.0 $\mu\Omega$ cm, respectively, so that RRR$\equiv \rho(300\ \mathrm{K})/\rho(40\ \mathrm{K})$, was 5.8. ρ under H did not change appreciably so that MR $\equiv [\rho(T,H)-\rho(T,H=0)]/\rho(T,H=0)$ at $T=40$ K is less

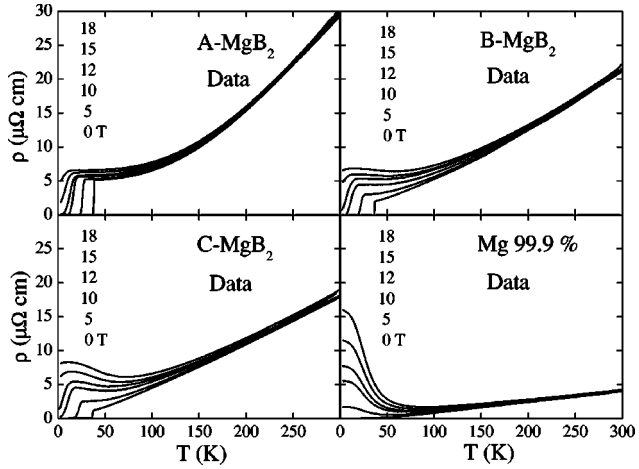

FIG. 1. *T*- and *H*-dependent resistivity ρ curves for *A*-, *B*-, *C*-MgB_2 and Mg (Alfa Aesar #43355). The quantitiy of unreacted Mg was increasing in the order of *A*-, *B*-, and *C*-MgB_2.

than 10% for $H \leqslant 10$ T. This relatively small MR value is consistent with the results of many polycrystalline[9] as well as single crystalline MgB_2 samples, for which $4.5 \lesssim \mathrm{RRR} \lesssim 6$.[11] Magnetization measurements also showed that *A*-MgB_2 has the highest $T_c \simeq 39$ K and the smallest $\Delta T_c \simeq 0.5$ K. These results, combined with the SEM and XRD studies, suggest that *A*-MgB_2 is a highly stoichiometric sample.

On the other hand, $\rho(T,H=0)$ values of *B*-MgB_2 and *C*-MgB_2 decrease significantly so that $\rho(40\ \mathrm{K}) = 2.12(1.29)\ \mu\Omega$ cm and $\rho(300\ \mathrm{K}) = 21.0(17.9)\ \mu\Omega$ cm for *B*-MgB_2 (*C*-MgB_2). $\rho(T,H=0)$ of both samples shows slightly lower values of $T_c \simeq 38.2$ K (*B*-MgB_2) and 38.0 K (*C*-MgB_2) and significantly larger $\Delta T_c \simeq 0.6$ (*B*-MgB_2) and 1.5 K (*C*-MgB_2). Due to the faster decrease of ρ at low *T*, RRR values become 9.90 and 13.9 for *B*-MgB_2 and *C*-MgB_2, respectively. The increasing RRR value is correlated with increasing MR at low temperatures,[8] and more linear *T* dependence of $\rho(T)$ in our samples. For example, MR values at $T=40$ K and $H=18$ T changed from 30% (*A*-MgB_2) to 226% (*B*-MgB_2) and 452% (*C*-MgB_2). The peculiar upturn behavior of $\rho(T,H)$, seen in *B*-MgB_2 and *C*-MgB_2 below 70 K, is a common feature observed in MgB_2 samples with large RRR values.[5]

To better understand the effects of Mg, we measured $\rho(T,H)$ of Mg metal. $\rho(T,H=0)$ was quite linear at $\sim 70 \leqslant T \leqslant 300$ K. At $T<70$ K, it is found that the data are well fit by $\rho(T,H=0) = \rho_0 + aT^3$ (a is a constant), indicating that electron-phonon scattering is dominant at low *T*. The ρ values at 40 and 300 K were 0.12 and 4.0 $\mu\Omega$ cm, respectively, so that RRR=34. Surprisingly, $\rho(T,H)$ at $H \neq 0$ show a drastic increase below ~ 70 K. For example, $\rho(3\ \mathrm{K}, 18\ \mathrm{T})$ is almost three orders of magnitude larger than $\rho(3\ \mathrm{K}, H=0)$.

In the literature, it is well known that the divalent Mg metal shows a nonsaturating large transverse MR, because most electron trajectories of Mg on the Fermi surface close within one or more cells of the reciprocal lattice with volume compensation of electrons and holes.[13,14] However, some parts of the Fermi surface of Mg under certain orientations of magnetic field can produce open trajectories of electrons, which are prone to magnetic breakdown in sufficiently high *H*. Due to the presence of open orbits, $\rho(H)$ of Mg is found to be increasing as H^t with $1.5 \lesssim t < 2$, and the transverse MR becomes very sensitive to the crystal orientation and geometry of a sample at low $H < \sim 10$ T.[13] In the higher-field limit, with magnetic breakdown of most open orbits, $\rho(H)$ of Mg is expected to largely recover the H^2 behavior of closed orbits.

Consistent with this picture, our data of polycrystalline Mg at $H \geqslant 12$ T can be well explained by the equation for a simple metal under a magnetic field, i.e., $\rho(T,H) = \rho(T,0) \times \{1 + (\omega_c \tau)^2\} = \rho(T,0)\{1 + b(H/\rho(T,0))^2\}$, with $\omega_c = eH/m^*c$ and a constant b.[14] Based on this formula, the peculiar upturn in $\rho(T,H>0)$ below ~ 70 K can be understood in terms of the crossover from the high-*T*–thermal-phonon $[\rho(T,0) \propto T]$ to the low *T*–electron-phonon $[\rho(T,0) = \rho_0 + aT^3]$ scattering regime. At a fixed *H*, as *T* is decreased, the *T* dependence of the MR will dramatically increase (roughly from $\propto T^{-2}$ to $\propto T^{-6}$) at this crossover. Note, furthermore, that the *T* dependence of the MR will saturate in the zero *T*-limit when $\rho(T) \sim \rho_0$, consistent with our lowest temperature-Mg data.

In Fig. 1, it is interesting to note that the low *T*-upturn behavior of $\rho(T,H>0)$ of Mg metal is quite similar to that seen in *B*-MgB_2 and *C*-MgB_2. This observation strongly suggests that the enhanced MR and RRR of *B*-MgB_2 and *C*-MgB_2 could be due to Mg embedded in those samples. Note also that the small low-*T* resistivity of Mg is consistent with the systematic decrease of ρ from *A*-MgB_2 to *B*-MgB_2 to *C*-MgB_2. To quantitatively check this postulation, we calculated the resistivity expected from two-phase samples consisting of MgB_2 and Mg, based on the generalized effective medium (GEM) theory developed by McLachlan.[15] If we assume that *B*-MgB_2 and *C*-MgB_2 are isotropic phase mixtures, mainly composed of the MgB_2 and Mg grains, the GEM equation predicts the effective resistivity ρ_E of the binary phase mixture as

$$(1-f)\left(\frac{\rho_1^{-1/t} - \rho_E^{-1/t}}{\rho_1^{-1/t} + A\rho_E^{-1/t}}\right) + f\left(\frac{\rho_2^{-1/t} - \rho_E^{-1/t}}{\rho_2^{-1/t} + A\rho_E^{-1/t}}\right) = 0, \quad (1)$$

where $A = (1-f_c)/f_c$. Here, the critical volume fraction f_c and critical exponent *t* are close to 0.17 and 2 in three dimensions. When resistivity values of the components ρ_1 and ρ_2 and the volume fraction of the second component, *f*, are known, this equation successfully predicted ρ_E of various inhomogeneous media[16] as well as electronically phase-separated manganites,[17] in wide *f* ranges including the percolation regime.

To calculate $\rho_E(T,H)$ from Eq. (1), we set $\rho_1(T,H)$ and $\rho_2(T,H)$ equal to the data from *A*-MgB_2 and Mg, respectively. Figure 2 shows the simulated $\rho_E(T,H)$ results at fixed *f*. The curves with $f = 0.05$–0.30 well represent main features of $\rho(T,H)$ of *B*-MgB_2 and *C*-MgB_2: a systematic decrease of ρ, a quasilinear *T* dependence at $H=0$, and than upturn behavior at high fields. Furthermore, even with small $f < 0.05$, MR values become significant at low *T*. Therefore,

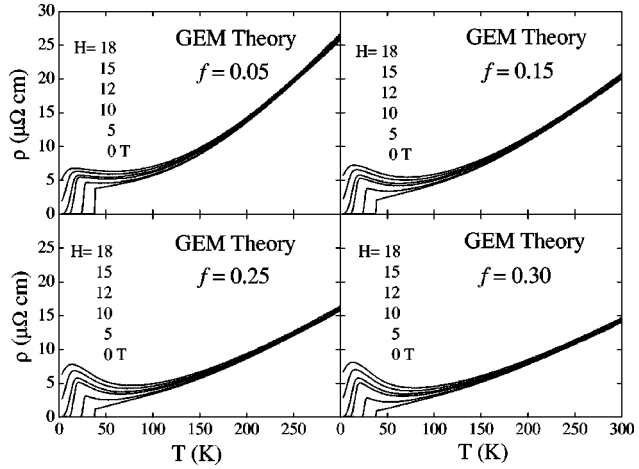

FIG. 2. Predicted ρ curves by the generalized-effective-medium (GEM) theory at several Mg volume fractions f, when two ingredients are assumed to be Mg and A-MgB_2.

$\rho(T,H)$ curves of B-MgB_2 and C-MgB_2 are well explained qualitatively by the simulation results in Fig. 2.[18] On the other hand, a strict comparison of the $\rho(T,H)$ curves was imperfect: the experimental values were, in general, slightly larger than the simulated ones, and showed a steeper increase with T. This discrepancy in absolute resistivity might be due to the presence of other insulating impurities such as MgO and B_2. An alternative way to make a quantitative comparison to the GEM theory is to focus on *relative* physical quantities such as RRR and MR, because they are dominated by conducting phases and, thus, will not be affected by the presence of small quantities of insulating phases.

Figure 3(a) shows a calculated RRR vs f curve of $\rho_E(T,H)$. The RRR values at $f=0.0$ and 1.0 correspond to 5.8 (RRR of A-MgB_2) and 34 (RRR of Mg), respectively. For the RRR values of B-MgB_2, 9.9, and C-MgB_2, 13.8, the calculated curve predicts that $f=0.17$ and 0.30 for B-MgB_2 and C-MgB_2, respectively. The predicted MR vs f curve at $H=18$ T and $T=40$ K [right axis of Fig. 3(a)] can also be calculated from Eq. (1). At the predicted $f=0.17$ and 0.30, the calculated MR curve predicts MR values of 220% and 470 %, respectively. These values are in very good agreement with the experimental MR data of B-MgB_2 (+) and C-MgB_2 (×), 220% and 460 %, respectively. This level of quantitative agreement confirms that the two-phase analysis provides an accurate modeling of the relative physical quantities RRR and MR.

To check this agreement at various temperatures, we plot predicted MR vs RRR curves at 40, 50, and 60 K in Fig. 3(b). The experimental MR values at $H=18$ T of B-MgB_2 and C-MgB_2, shown as + and ×, well match the curves predicted by Eq. (1) within error bars. We verified that this agreement is valid at the other temperatures above T_c. All of these results unequivocally show that two important physical quantities, RRR and MR of MgB_2 with excess Mg are intimately linked to each other, and that they are determined by the properties of Mg itself. As a result, we estimate the Mg volume fractions embedded inside samples B-MgB_2 and C-MgB_2 to be $f=0.17$ and 0.30, respectively. It is noted that

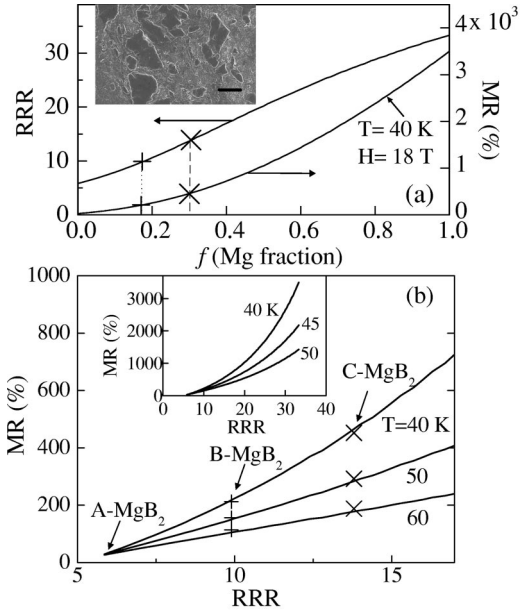

FIG. 3. (a) The GEM equation predictions for MR and RRR as a function of f. Symbols + and × represent the experimental RRR and MR values of B-MgB_2 and C-MgB_2, respectively, from which we estimate $f\simeq 0.17$ for B-MgB_2 and $f\simeq 0.30$ for C-MgB_2. The inset shows a SEM image of sample C with ~29 % of a total area as Mg islands (black). The scale bar represents 100 μm. (b) Correlation in the GEM theory between RRR and MR at 40, 50, and 60 K (solid lines). Symbols + and × represent the experimental MR values of B-MgB_2 and C-MgB_2, respectively. The inset shows the calculated MR vs RRR curve over a wider range of RRR.

these f values are quite consistent with the observed Mg areas in the SEM pictures of B-MgB_2 and C-MgB_2, confirming the validity of the GEM analyses.

The inset of Fig. 3(b) illustrates that the simulated MR vs RRR curves are roughly quadratic. More precisely, the simulated MR vs RRR curves at $40\leqslant T\leqslant 50$ K have a power law relation $MR\propto(RRR)^t$ with $t\approx 1.9$–2.4. A similar power law relationship of $MR\propto(RRR)^{2.2}$ at $T=50$ K was empirically found in a previous report that studied $\rho(T,H)$ up to 5 T in $Mg_{1+\delta}B_2$ samples.[8] This report in the literature can be successfully explained by Eq. (1), confirming that the RRR and MR behaviors of Mg can be attributed to those of MgB_2 samples with excess Mg.

As a final quantitative comparison, in Figs. 4(b) and 4(d) we plot the curves of MR vs T from Eq. (1) with fixed $f=0.17$ and 0.30 at various value of H. Experimental curves of MR of B-MgB_2 and C-MgB_2 are shown in Figs. 4(a) and 4(c), respectively. The agreement between theoretical curves and experimental data is satisfactory at high $H\geqslant 12$ T. At lower H of 5 and 10 T, the theoretical MR values become somewhat larger than experimental ones, a discrepancy that might well be related to the same magnetic breakdown effects that make Mg sensitive to domain size and orientation at low H.[13,14] A complete understanding of the role of the magnetic breakdown effect on the physical properties of impure MgB_2 would be exceedingly difficult, requiring a detailed knowledge of the orientations of the Mg metal grains.

All of the above experimental findings demonstrate that

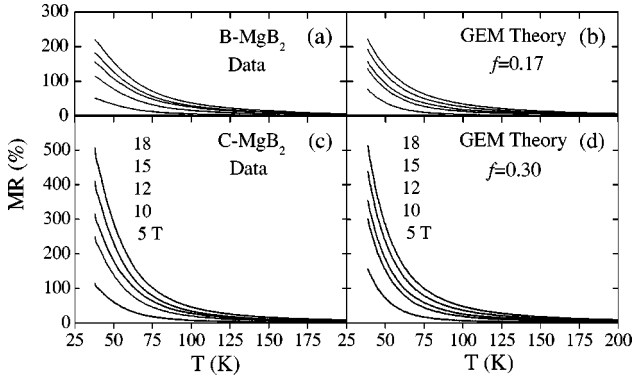

FIG. 4. Experimental MR data of (a) B-MgB_2 and (c) C-MgB_2 above T_C. The GEM theory for MR with (b) $f=0.17$ and (d) $f=0.30$, which quantitatively accounts for the MR data of B-MgB_2 and C-MgB_2, respectively.

the existence of a small amount of Mg inside MgB_2 samples can significantly affect magnetotransport properties. The diversity of magnetotransport properties of MgB_2 reported in the literature can be qualitatively understood by Mg nonstoichiometry, as indicated by the simulation results of Figs. 2–4. We identify low residual resistivity and a drastic increase of RRR and MR as due to Mg metal forming a two-phase system with MgB_2. With this understanding, then, a large RRR and low residual resistivity can no longer be criteria for a stoichiometric MgB_2 sample. According to our experimental findings and single-crystal studies,[11] the RRR of stoichiometric MgB_2 is suggested to be $\sim 5-7$. Our study also finds that artificial inclusion of excess Mg into MgB_2 can be used to reduce the overall normal-state resistivity of the composite, a result which, for example, could improve the quench characteristics of superconducting MgB_2 wires.[4]

In conclusion, we systematically investigated the effect of Mg metal on the magnetotransport properties of MgB_2. Electrical transport of MgB_2 is found to depend sensitively on the amount of Mg in the sample. Generalized effective-medium theory quantitatively accounts for the behavior of the relative transport properties of magnetoresistance and residual resistance ratio, establishing that MgB_2 samples with unreacted Mg form a two-phase mixture of MgB_2 and Mg metal. This study highlights the importance of Mg stoichiometry in understanding transport properties and developing technological applications of the new superconductor MgB_2.

We appreciate valuable discussions with Dr. C. M. Varma, Professor Y. Bang, and Dr. S. P. Chen. The work at NHMFL was performed under the auspices of the National Science Foundation, the State of Florida, and the U. S. Department of Energy. This work was also supported by the Ministry of Science and Technology of Korea through the Creative Research Initiative Program.

[1] Jun Nagamatsu, N. Nakagawa, T. Muranaka, Y. Zenitana, and J. Akimitsu, Nature (London) **410**, 63 (2001).

[2] S.L. Bud'ko, G. Lapertot, C. Petrovic, C.E. Cunningham, N. Anderson, and P.C. Canfield, Phys. Rev. Lett. **86**, 1877 (2001).

[3] See for a review, C. Buzea and T. Yamashita, Supercond. Sci. Technol. **14**, R115 (2001).

[4] P.C. Canfield, D.K. Finnemore, S.L. Bud'ko, J.E. Ostenson, G. Lapertot, C.E. Cunningham, and C. Petrovic, Phys. Rev. Lett. **86**, 2423 (2001).

[5] D.K. Finnemore, J.E. Ostenson, S.L. Bud'ko, G. Lapertot, and P.C. Canfield, Phys. Rev. Lett. **86**, 2420 (2001); S.L. Bud'ko, C. Petrovic, G. Lapertot, C.E. Cunningham, P.C. Canfield, M.H. Jung, and A.H. Lacerda, Phys. Rev. B **63**, 220503 (2001).

[6] M.H. Jung, M. Jaime, A.H. Lacerda, G.S. Boebinger, W.N. Kang, H.-J. Kim, E.-M. Choi, and S.-I. Lee, Chem. Phys. Lett. **343**, 447 (2001).

[7] C.U. Jung, Min-Seok Park, W.N. Kang, Mun-Seog Kim, Kijoon H.P. Kim, S.Y. Lee, and Sung-Ik Lee, Appl. Phys. Lett. **78**, 4157 (2001).

[8] X.H. Chen, Y.S. Wang, Y.Y. Xue, R.L. Meng, Y.Q. Wang, and C.W. Chu, Phys. Rev. B **65**, 024502 (2001).

[9] G. Fuchs, K.-H. Müller, A. Handstein, K. Nenkov, V.N. Narozhnyi, D. Eckert, M. Wolf, and L. Shultz, Solid State Commun. **118**, 497 (2001); N.A. Frederick, S. Ki, M.B. Maple, V.F. Nesterenko, and S.S. Indrakanti, Physica C **363**, 1 (2001); P. Szabo, P. Samuely, A.G.M. Jansen, T. Klein, J. Marcus, D. Fruchart, and S. Miraglia, *ibid.* **369**, 250 (2002).

[10] L.R. Testardi, J.M. Poate, and H.J. Levinstein, Phys. Rev. B **15**, 2570 (1977).

[11] M. Xu, H. Kitazawa, Y. Takano, J. Ye, K. Nishida, H. Abe, A. Matsushita, and G. Kido, Appl. Phys. Lett. **79**, 2779 (2001); Kijoon H.P. Kim, J.-H. Choi, C.U. Jung, P. Chowdhury, H.-S. Lee, M.-S. Park, H.-J. Kim, J.Y. Kim, Z. Du, E.-M. Choi, M.-S. Kim, W.N. Kang, S.-I. Lee, G.Y. Sung, and J.Y. Lee, Phys. Rev. B **65**, 100510 (2002); S. Lee, H. Mori, T. Masui, Yu. Eltsev, A. Yamamoto, and S. Tajima, J. Phys. Soc. Jpn. **70**, 2255 (2001).

[12] C.U. Jung *et al.*, Physica C (to be published).

[13] R.W. Stark, T.G. Eck, and W.L. Gordon, Phys. Rev. **133**, A443 (1964); F. Richards, Phys. Rev. B **8**, 2552 (1973); R.W. Stark and R. Reifenberger, J. Low Temp. Phys. **26**, 763 (1977).

[14] A.B. Pippard, *Magnetoresistance in Metals* (Cambridge Univ. Press, New York, 1988).

[15] D.S. McLachlan, J. Phys. C **20**, 865 (1987).

[16] G. Hurvits, R. Rosenbaum, and D.S. McLachlan, J. Appl. Phys. **73**, 7441 (1993), and references therein.

[17] K.H. Kim, M. Uehara, C. Hess, P.A. Sharma, S.-W. Cheong, Phys. Rev. Lett. **84**, 2961 (2000).

[18] Saturation of high-field ρ values below 10 K, observed in B-MgB_2 and C-MgB_2, is not reproduced in the calculated curves of Fig. 2, which can be related to H_{c2} (3 K)$\approx$8.5 T of C-MgB_2, 10.5 T of B-MgB_2, and 13 T of A-MgB_2. Excess Mg may also influence the intrinsic properties of MgB_2 grains to change H_{c2}, T_c, and ΔT_c.